Bioprocess and Biosystems Engineering (2021) 44:1755–1768
https://doi.org/10.1007/s00449-021-02558-y

RESEARCH PAPER

State estimation and nonlinear tracking control simulation approach. Application to a bioethanol production system

M. Cecilia Fernández[1] · M. Nadia Pantano[1] · Leandro Rodriguez[1] · Gustavo Scaglia[1]

Received: 13 February 2020 / Revised: 20 April 2020 / Accepted: 8 May 2020 / Published online: 16 May 2021

Abstract

Tracking control of specific variables is key to achieve a proper fermentation. This paper analyzes a fed-batch bioethanol production process. For this system, a controller design based on linear algebra is proposed. Moreover, to achieve a reliable control, on-line monitoring of certain variables is needed. In this sense, for unmeasurable variables, state estimators based on Gaussian processes are designed. Cell, ethanol and glycerol concentrations are predicted with only substrates measurement. Simulation results when the controller and estimators are coupled, are shown. Furthermore, the algorithms were tested with parametric uncertainties and disturbances in the control action, and are compared, in all cases, with neural networks estimators (previous work). Bayesian estimators show a performance improvement, which is reflected in a decrease of the total error. Proposed techniques give reliable monitoring and control tools, with a low computational and economic cost, and less mathematical complexity than neural network estimators.

Keywords On-line monitoring · Profiles tracking control · Fed-batch bioprocess · Non-linear and multivariable system · State estimation · Gaussian process

Introduction

Nowadays, ethanol plays an extremely important role in the industry. Because of its excellent capacity as solvent, it is used in cosmetics, paints, cleaning products, extracts, and medicines. In aerosols, ensures the adhesion of the material on the different surfaces. It is the raw material for biodiesel production. Its use in gasoline favors fuel oxygenation, and as a fuel, it is less toxic, easily biodegradable and produces fewer pollutants. Its antiseptic properties make it an indispensable complement to achieve the conservation of lotions, syrups, and foods, besides, it promotes the uniform distribution of pigments and enhances flavors. Finally, it constitutes an essential input in hospitals, homes, etc. [1].

Ethanol can be obtained by ethylene hydration (derived from petroleum), or, from renewable materials fermentation. Excessive consumption of fossil fuels has led to a decrease in these natural resources and pollution of the environment [2, 3]. Some of the most visible consequences are global warming, acid rain and urban smog [4]. For this reason, non-polluting and renewable fuels have become a focus of research in recent years.

Bioethanol (from renewable resources) production involves different stages: pretreatment, hydrolysis, fermentation, and distillation. Consequently, this process uses a significant amount of energy compared to fossil fuel processing, so it is not possible to completely replace current oil consumption. As a result, it is necessary to guide research to optimize and control each stage of the bioethanol production process. Many researchers have dedicated their efforts to achieve this, for example, Herrero et al. [5] presented the optimization results of the sulfuric acid pretreatment variables applied to improve sugars bioavailability. In Aimaretti et al. [6], authors studied two different enzymatic hydrolysis strategies to increase fermentable sugar concentration in the must. Kumar et al. [7], increase the efficiency of sugar

✉ M. Cecilia Fernández
mcfernandez@unsj.edu.ar

M. Nadia Pantano
npantano@unsj.edu.ar

Leandro Rodriguez
lrodri@unsj.edu.ar

Gustavo Scaglia
gscaglia@unsj.edu.ar

[1] Instituto de Ingeniería Química, Universidad Nacional de San Juan (UNSJ), CONICET, Av. Lib. San Martín Oeste 1109, J5400ARL San Juan, Argentina

conversion and the ethanol yield of a fermentation applying gas stripping at high temperature. In Tgarguifa et al. [8], the model and a distillation column optimization to produce ethanol from wine are proposed.

The fermentation step, commonly done in batch or fed-batch bioreactors, can be improved with many strategies, such as the specific microorganism selection or genetic modification of those microorganisms [1, 4]. Fed-batch bioprocesses are intensively studied nowadays because of their complex mathematical models [9] and their main advantages [10], such as the medium substrate concentration can be regulated by an appropriate feed rate profile [11], obtaining better production yields and minimizing the production costs [10, 12–14]. Run-to-run optimization is a current method used to define the process feed flow rate and system parameters. Moreover, this strategy is used for open-loop control purposes, however, thus lead to performance deterioration in each run [15, 16]. In this way, bioprocesses tracking control is a more robust option, required to follow certain optimal feed flow rate, get stability and the best productivity [17]. Moreover, a real-time bioprocess detailed control is a complex target but is essential to ensure raw materials optimal use, water and energy-saving, final product consistent quality, a reduction in wastes and process cycle time, which opens up the possibility of bioprocess innovation. Furthermore, the mathematical representation of the process and the on-line states variables measurement are keys to achieve good results [15].

Many scientists have developed several feedback control strategies. However, to the best of the author's knowledge, for the specific case of fed-batch bioethanol production defined by Hunag et al. [18], only Fernández et al. [19] presented a controller design. It is focused on looking for control actions, to track predefined concentration profiles. This methodology is complemented with on-line state estimators based on neural networks (NN) to provide information on those variables that cannot be measured on-line. As the controller structure comes from the process mathematical model, it can be implemented in many systems. This procedure is simple, versatile and precise. Besides, only basic knowledge of numerical methods and linear algebra are needed to implement it. The technique was tested against different disturbances, achieving the tracking error convergence to zero.

In this paper, another alternative for non-measurable variables estimation in the same bioethanol production system is presented. In this sense, Bayesian theory based on Gaussian Processes are used to estimate cell, ethanol and glycerol concentrations. With this alternative, in comparison with NN, fewer parameters are involved, simplifying the mathematical resolution of the problem, reducing the programming time and minimizing the computational cost. Furthermore, the controller parameters are selected with a Monte Carlo Randomized algorithm and a comparison with the NN state estimators, previously presented [19], is shown, under parametric uncertainties and external perturbation addition.

The paper is organized as follows. Section "Bioprocess model and controller design" summarizes the ethanol bioprocess and the previously presented controller technique. In Section "Bayesian state estimators design", the state estimators are developed. Section Results and discussion shows the results and discussion, including a comparison of the controller performance using the NN and the Bayesian state estimators. Finally, conclusions are exposed.

Bioprocess model and controller design

Ethanol bioprocess description

Hunag et al. [18], proposed the following mathematical model to describe a fed-batch bioethanol process:

$$\begin{cases} \dfrac{\mathrm{d}X}{\mathrm{d}t} = (\mu_1 + \mu_2)X - \dfrac{U}{V}X \\ \dfrac{\mathrm{d}S_1}{\mathrm{d}t} = -\left(\dfrac{q_{S_1/P_1}}{Y_{P_1/S_1}} + \dfrac{q_{S_1/P_2}}{Y_{P_2/S_1}}\right)X + \dfrac{U}{V}\left(\lambda S_\mathrm{f} - S_1\right) \\ \dfrac{dS_2}{\mathrm{d}t} = -\left(\dfrac{q_{S_2/P_1}}{Y_{P_1/S_2}} + \dfrac{q_{S_2/P_2}}{Y_{P_2/S_2}}\right)X + \dfrac{U}{V}\left((1-\lambda)S_\mathrm{f} - S_2\right) \\ \dfrac{\mathrm{d}P_1}{\mathrm{d}t} = -\left(q_{S_1/P_1} + q_{S_2/P_1}\right)X + \dfrac{U}{V}P_1 \\ \dfrac{\mathrm{d}P_2}{\mathrm{d}t} = -\left(q_{S_1/P_2} + q_{S_2/P_2}\right)X + \dfrac{U}{V}P_2 \end{cases} \quad (1)$$

where:

$$\begin{aligned} \frac{\mathrm{d}V}{\mathrm{d}t} &= U \\ \mu_1 &= \frac{\mu_{m_1} S_1}{K_{S_1} + S_1 + S_1^2/K_{S_{1I}}} \frac{K_{P_1}}{K_{P_1} + P_1 + P_1^2/K_{P_{1I}}} \\ \mu_2 &= \frac{\mu_{m_2} S_2}{K_{S_2} + S_2 + S_2^2/K_{S_{2I}}} \frac{K_{P_2}}{K_{P_2} + P_1 + P_1^2/K_{P_{2I}}} \\ q_{S_1/P_1} &= \frac{\nu_{S_1P_1} S_1}{K_{S_1P_1} + S_1} \frac{k_{S_1P_1}}{k_{S_1P_1} + P_1} \\ q_{S_2/P_2} &= \frac{\nu_{S_2P_2} S_2}{K_{S_2P_2} + S_2} \frac{k_{S_2P_2}}{k_{S_2P_2} + P_2} \\ q_{S_1/P_2} &= \frac{\nu_{S_1P_2} S_1}{K_{S_1P_2} + S_1} \frac{k_{S_1P_2}}{k_{S_1P_2} + P_2} \\ q_{S_2/P_1} &= \frac{\nu_{S_2P_1} S_2}{K_{S_2P_1} + S_2} \frac{k_{S_2P_1}}{k_{S_2P_1} + P_1}. \end{aligned} \quad (2)$$

The microorganism used is a high tolerance to high ethanol concentration yeast, *Saccharomyces diastaticus* (X). This

yeast uses two substrates, glucose (S_1) and fructose (S_2), which are fed into the reactor in a 50–50 ratio, to produce ethanol (P_1) and glycerol (P_2). The states are: (X), (S_1), (S_2), (P_1) and (P_2) concentration inside the reactor, whose profiles variation over time is wanted to be tracked. V is the culture volume, μ_1 and μ_2 are the specific yeast cells growth rate, $q_{S1/P1}$ and $q_{S2/P1}$ the specific ethanol production rate, $q_{S1/P2}$ and $q_{S2/P2}$ the specific glycerol production rate, in all cases from glucose and fructose, respectively. U is the feed rate and the control variable.

Table 1 Initial conditions for ethanol fermentation

Variable	Initial value
X (g/L)	1.5
P_1 (g/L)	5.3
P_2 (g/L)	0.0001
S_1 (g/L)	8.6
S_2 (g/L)	8.6
V (L)	1.35

To estimate kinetic model parameters, fed glucose concentration, feed strategy and fermentation time to maximize the ethanol production rate, Hunag et al. [18] applied a run-to-run optimization procedure. Those results are used as references in this paper. A reactor with a total working volume of 5 L was used. Temperature was maintained at 35.8 °C by controlling the circulation of the cooling water. The airflow was fixed at 1.5 vvm, and the pH was kept at 5.0 by adding 1 N NaOH. The biomass concentration was determined spectrophotometrically at 540 nm, and the corresponding dry weight of cells was obtained from a calibration curve. The concentrations of glucose, fructose, ethanol and glycerol were analyzed with a high-performance liquid chromatograph [18]. Table 1 shows system initial conditions, while parameters nomenclature, description and values are exposed in Table 2.

Controller design

The methodology described in Fernández et al. [19] aims to find U in order to make the system follow pre-established state

Table 2 Nomenclature, description and values of parameters

Parameter	Description	Value
μ_{m1}	Maximum specific growth rate coefficient for yeast on glucose (/h)	1.8823
μ_{m2}	Maximum specific growth rate coefficient for yeast on fructose (/h)	1.7098
$Y_{P1/S1}$	Yield coefficient for ethanol from glucose	0.5085
$Y_{P2/S1}$	Yield coefficient for glycerol from glucose	0.5331
$Y_{P1/S2}$	Yield coefficient for ethanol from fructose	0.5098
$Y_{P2/S2}$	Yield coefficient for glycerol from fructose	0.4462
K_{S1}	Saturation coefficient for cell growth on glucose (g/L)	159.75
K_{S1I}	Inhibition coefficient for cell growth on glucose (g/L)	94.233
K_{P1}	Saturation coefficient for cell growth on ethanol (g/L)	238.39
K_{P1I}	Inhibition coefficient for cell growth on ethanol (g/l)	2.7378
K_{S2}	Saturation coefficient for cell growth on fructose (g/L)	0.0726
K_{S2I}	Inhibition coefficient for cell growth on fructose (g/L)	9.0048
K_{P2}	Saturation coefficient for cell growth on glycerol (g/L)	35.958
K_{P2I}	Inhibition coefficient for cell growth on glycerol (g/L)	9.9722
K_{S1P1}	Saturation coefficient for ethanol production on glucose (g/L)	1.3409
k_{S1P1}	Inhibition coefficient for ethanol production on glucose (g/L)	18.612
K_{S2P1}	Saturation coefficient for ethanol production on fructose (g/L)	0.9129
k_{S2P1}	Inhibition coefficient for ethanol production on fructose (g/L)	1000
K_{S1P2}	Saturation coefficient for glycerol production on glucose (g/L)	6.7116
k_{S1P2}	Inhibition coefficient for glycerol production on glucose (g/L)	0.5863
K_{S2P2}	Saturation coefficient for glycerol production on fructose (g/L)	0.4310
k_{S2P2}	Inhibition coefficient for glycerol production on fructose (g/L)	1.150
ν_{S1P1}	Coefficient of maximum specific ethanol production rate for yeast on glucose (/h)	1.5051
ν_{S2P1}	Coefficient of maximum specific ethanol production rate for yeast on fructose (/h)	0.3321
ν_{S1P2}	Coefficient of maximum specific glycerol production rate for yeast on glucose (/h)	0.0023
ν_{S2P2}	Coefficient of maximum specific glycerol production rate for yeast on fructose (/h)	0.1609
λ	Proportion of glucose and fructose	0.5
S_f	Sugar total feed concentration (g/L)	300

variables profiles (references) with minimum error. For the controller, design is assumed that reference profiles and states at each sampling instant are known. Figure 1 shows the reference concentration profiles and the feed flow rate. Next, the mentioned methodology is summarized:

First, Eq. (1) is discretized using numerical methods. Euler is applied due to its simplicity and good results [19].

$$\left(\frac{\mathrm{d}\sigma}{\mathrm{d}t}\right) = \frac{\sigma_{n+1} - \sigma_n}{T_\mathrm{S}}, \tag{3}$$

where σ symbolizes each state variable, σ_n is the current σ value measured from the reactor (on-line), and σ_{n+1} is the σ value in the next measurement instant. T_S is the sampling time (0.1 h) [20]. The process lasts *15.7 h* (T_f).

The state variables in $n+1$ are approximated as follows:

$$\begin{aligned} &\underbrace{\sigma_{\mathrm{ref},n+1} - \sigma_{n+1}}_{\mathrm{error}_{n+1}} = k_\sigma \underbrace{(\sigma_{\mathrm{ref},n} - \sigma_n)}_{\mathrm{error}_n} \\ &\sigma_{n+1} = \sigma_{\mathrm{ref}\,n+1} - k_\sigma(\sigma_{\mathrm{ref},n} - \sigma_n) \end{aligned} \tag{4}$$

Here, σ_{ref} are the reference state variables. k_σ represents the controller parameter for the variable σ. For this system, the controller parameters are k_X, k_{P1}, k_{P2}, k_{S1} and k_{S2}. For the error reduction in each sampling time, $0 \le k_\sigma < 1$must be fulfilled. Then, replacing Eq. (4) in (3):

$$\left(\frac{\mathrm{d}\sigma}{\mathrm{d}t}\right) = \frac{\overbrace{\left[\sigma_{\mathrm{ref}\,n+1} - k_\sigma(\sigma_{\mathrm{ref}\,n} - \sigma_n)\right]}^{\sigma_{n+1}} - \sigma_n}{T_\mathrm{S}} = \frac{\Delta\sigma}{T_\mathrm{S}}. \tag{5}$$

Placing Eq. (5) in (1):

$$\begin{cases} \dfrac{\Delta X}{T_\mathrm{S}} = (\mu_1 + \mu_2)X_n - \dfrac{U_n}{V_n}X_n \\ \dfrac{\Delta S_1}{T_\mathrm{S}} = -\left(\dfrac{q_{S_1/P_1}}{Y_{P_1/S_1}} + \dfrac{q_{S_1/P_2}}{Y_{P_2/S_1}}\right)X_n + \dfrac{U_n}{V_n}(\lambda S_\mathrm{f} - S_{1,n}) \\ \dfrac{\Delta S_2}{T_\mathrm{S}} = -\left(\dfrac{q_{S_2/P_1}}{Y_{P_1/S_2}} + \dfrac{q_{S_2/P_2}}{Y_{P_2/S_2}}\right)X_n + \dfrac{U_n}{V_n}((1-\lambda)S_f - S_{2,n}) \cdot \\ \dfrac{\Delta P_1}{T_\mathrm{S}} = (q_{S_1/P_1} + q_{S_2/P_1})X_n - \dfrac{U_n}{V_n}P_{1,n} \\ \dfrac{\Delta P_2}{T_\mathrm{S}} = (q_{S_1/P_2} + q_{S_2/P_2})X_n - \dfrac{U_n}{V_n}P_{2,n} \end{cases} \tag{6}$$

Expressing (6) in vector form, it is obtained:

$$\overbrace{\begin{bmatrix} -X_n/V_n \\ (\lambda S_f - S_{1,n})/V_n \\ ((1-\lambda)S_\mathrm{f} - S_{2,n})/V_n \\ -P_{1,n}/V_n \\ -P_{2,n}/V_n \end{bmatrix}}^{A} \overbrace{U_n}^{u} = \overbrace{\begin{bmatrix} \dfrac{\Delta X}{T_\mathrm{S}} - (\mu_1 + \mu_2)X_n \\ \dfrac{\Delta S_1}{T_\mathrm{S}} + \left(\dfrac{q_{S_1/P_1}}{Y_{P_1/S_1}} + \dfrac{q_{S_1/P_2}}{Y_{P_2/S_1}}\right)X_n \\ \dfrac{\Delta S_2}{T_\mathrm{S}} + \left(\dfrac{q_{S_2/P_1}}{Y_{P_1/S_2}} + \dfrac{q_{S_2/P_2}}{Y_{P_2/S_2}}\right)X_n \\ \dfrac{\Delta P_1}{T_\mathrm{S}} - (q_{S_1/P_1} + q_{S_2/P_1})X_n \\ \dfrac{\Delta P_2}{T_\mathrm{S}} - (q_{S_1/P_2} + q_{S_2/P_2})X_n \end{bmatrix}}^{b}$$

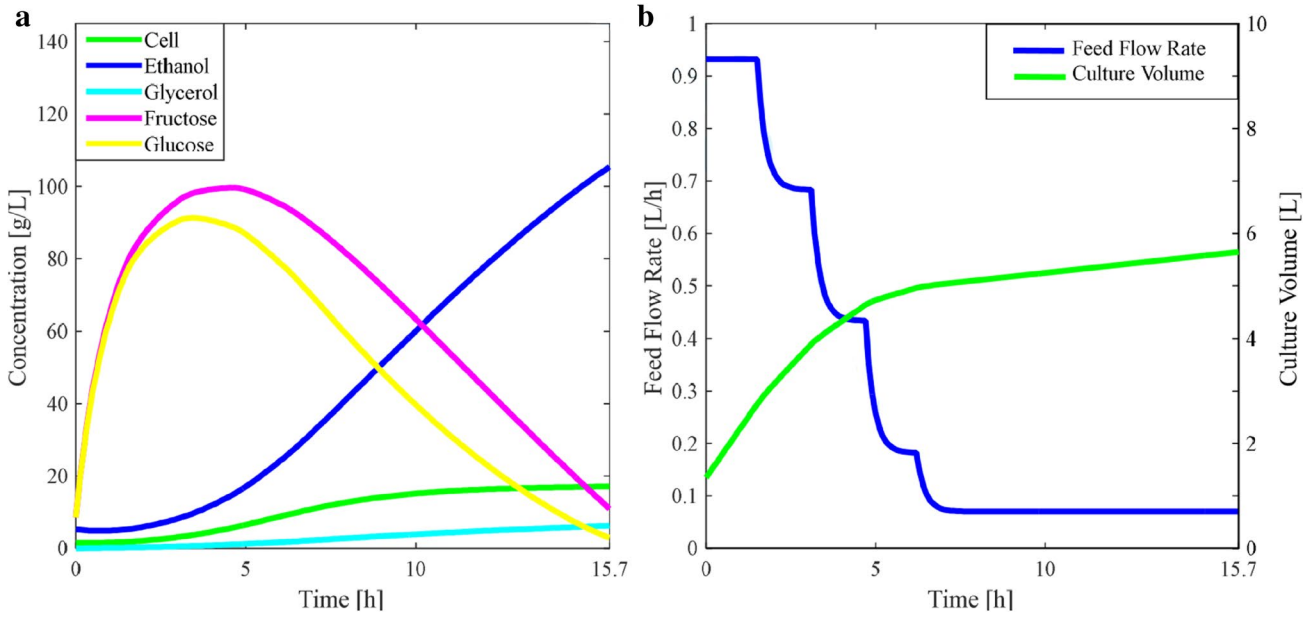

Fig. 1 **a** Cell, ethanol, glycerol, glucose and fructose reference concentrations along the process. **b** Reference feed flow rate. Culture Volume

Then, to find U, the equation system (7) must have an exact solution. So, **b** have to be a linear combination of **A** columns [21], in other words, **A** and **b** must be parallel. One way to satisfy this condition is:

$$\cos(A,b) = \frac{< A,b >}{||A|| * ||b||} = 1, \tag{8}$$

where the operation between $< >$ and $||.||$ represent the inner product and the vectors norm in R^n space, respectively.

At this point, a "sacrificed variable" selection is necessary. This variable, defined as S_{1ez}, ensures that (7) has an exact solution. For more details on its selection and calculation, see [19]. Finally, U_n is obtained using least squares.

$$U_n = \left(A^{\mathrm{T}}A\right)^{-1}A^{\mathrm{T}}b. \tag{9}$$

Controller tuning

In Fernández et al. [19], the Monte Carlo algorithm was used to find the k_σ combination that minimizes the accumulated error. This methodology consists of simulating the process N times using random k_σ [22]:

$$N \geq \left[\frac{\log\frac{1}{\delta}}{\log\frac{1}{1-\varepsilon}}\right], \tag{10}$$

where δ is the confidence and ε the accuracy.

Then, two new terms are introduced, "tracking error" and "total error", Eqs. (11) and (12), respectively.

$$\|e_n\| = \sqrt{\sum\left((\sigma_{\mathrm{ref},n} - \sigma_n)/\max\sigma_{\mathrm{ref},n}\right)^2}$$

$$E_{\mathrm{T}} = \sum\|e_n\|. \tag{12}$$

Equation (12) is the function cost to be minimized with the Monte Carlo Algorithm. Then, k_σ that minimize the total error are selected.

Sequence of the Monte Carlo algorithm [23]:

1. Define the controller's parameters to be optimized.
2. Determine the number of simulations to be performed (N). The values of δ and ε are chosen depending on the desired accuracy, for example: $\delta = 0.01$ and $\varepsilon = 0.005$, resulting in $N = 1000$.
3. A value is randomly assigned for each parameter of the controller.
4. The process is simulated and the cost index (E_{T}) is calculated.
5. Repeat steps 3 and 4 until completing the N iterations.
6. Finally, the controller parameters that minimize E_{T} are selected.

Theorem: *If the discrete system is given by Eq.* (1), *the control action is calculated with Eq.* (9), *and* k_σ *take values between zero and one* $(0 < k_\sigma < 1)$, *then, the tracking error convergence to zero when n tends to infinity is achieved.*

Demonstration Replacing the sacrificed variable in (7) and expressing the vector system generically:

$$\underbrace{\begin{bmatrix} a_1 \\ a_2 \\ a_3 \\ a_4 \\ a_5 \end{bmatrix}}_{\mathbf{A}} U_n = \underbrace{\begin{bmatrix} b_1 \\ b_2 \\ b_3 \\ b_4 \\ b_5 \end{bmatrix}}_{\mathbf{b}} \tag{13}$$

Solving (13) with least squares:

$$U_n = \left(A^{\mathrm{T}}A\right)^{-1}A^{\mathrm{T}}b = \frac{a_1b_1 + a_2b_2 + a_3b_3 + a_4b_4 + a_5b_5}{a_1^2 + a_2^2 + a_3^2 + a_4^2 + a_5^2}. \tag{14}$$

From (13):

$$\begin{aligned} \frac{a_1}{a_2} &= \frac{b_1}{b_2} \rightarrow b_2 = \frac{a_2}{a_1}b_1 \\ \frac{a_1}{a_3} &= \frac{b_1}{b_3} \rightarrow b_3 = \frac{a_3}{a_1}b_1 \\ \frac{a_1}{a_4} &= \frac{b_1}{b_4} \rightarrow b_4 = \frac{a_4}{a_1}b_1 \\ \frac{a_1}{a_5} &= \frac{b_1}{b_5} \rightarrow b_5 = \frac{a_5}{a_1}b_1. \end{aligned} \tag{15}$$

Replacing (15) in (14):

$$\begin{aligned} U_n &= \frac{a_1b_1 + \left(a_2^2b_1\right)/a_1 + \left(a_3^2b_1\right)/a_1 + \left(a_4^2b_1\right)/a_1 + \left(a_5^2b_1\right)/a_1}{a_1^2 + a_2^2 + a_3^2 + a_4^2 + a_5^2} \\ &= \frac{(b_1/a_1)\left(a_1^2 + a_2^2 + a_3^2 + a_4^2 + a_5^2\right)}{a_1^2 + a_2^2 + a_3^2 + a_4^2 + a_5^2} = \frac{b_1}{a_1} \\ &= \frac{V_n\left(\left(\left(X_{\mathrm{ref},n+1} - k_X\left(X_{\mathrm{ref},n} - X_n\right) - X_n\right)/T_{\mathrm{S}}\right) - \left(\mu_1\left(S_{1ez,n}, P_{1,n}\right) + \mu_2\left(S_{2,n}, P_{1,n}\right)\right)X_n\right)}{-X_n}. \end{aligned} \tag{16}$$

Substituting (16) in (7):

$$X_{n+1} = X_{\mathrm{ref},n+1} - k_X\left(X_{\mathrm{ref},n} - X_n\right) + T_S\left[\mu_1(S_{1ez,n}, P_{1,n}) - \mu_1(S_{1,n}, P_{1,n})\right]X_n. \tag{17}$$

Then, the tracking error for X is defined as:

$$e_{X,n+1} = X_{\mathrm{ref},n+1} - X_{n+1}. \tag{18}$$

Introducing (17) in (18):

$$e_{X,n+1} = k_X(X_{\mathrm{ref},n} - X_n) - T_S\left[\mu_1(S_{1ez,n}, P_{1,n}) - \mu_1(S_{1,n}, P_{1,n})\right]X_n. \tag{19}$$

The $\mu_1(S_{1n}, P_{1n})$ Taylor approximation in the desired value $\mu_1(S_{1ez\,n}, P_{1n})$ is:

$$\mu_1(S_{1,n}, P_{1,n}) = \mu_1(S_{1ez,n}, P_{1,n}) + \ldots + \left.\frac{\mathrm{d}\mu_1(S_1, P_{1,n})}{\mathrm{d}S_1}\right|_{S_1 = S_{ez,n} + \theta(S_{1,n} - S_{1ez,n}) = S_\theta} \left(S_{1n} - S_{1ez,n}\right), \tag{20}$$

where $0 < \theta < 1$.

Replacing (20) in (19):

$$e_{X,n+1} = k_X(X_{\mathrm{ref},n} - X_n) - T_S X_n \ldots \left[\mu_1(S_{1ez,n}, P_{1,n}) + \left.\frac{\mathrm{d}\mu_1(S_1, P_{1,n})}{\mathrm{d}S_1}\right|_{S_\theta} \underbrace{(S_{1n} - S_{1ez,n})}_{-e_{S_1,n}} - \mu_1(S_{1ez,n}, P_{1,n})\right] \times e_{X,n+1} = k_X(X_{ref,n} - X_n) + T_S \left.\frac{\mathrm{d}\mu_1(S_1, P_{1,n})}{\mathrm{d}S_1}\right|_{S_\theta} e_{S_1,n} X_n. \tag{21}$$

Proceeding in a similar way for the other variables and joining the final expressions:

$$\underbrace{\begin{bmatrix} e_{X,n+1} \\ e_{S_1,n+1} \\ e_{S_2,n+1} \\ e_{P_1,n+1} \\ e_{P_2,n+1} \end{bmatrix} = \begin{bmatrix} k_X & 0 & 0 & 0 & 0 \\ 0 & k_{S_1} & 0 & 0 & 0 \\ 0 & 0 & k_{S_2} & 0 & 0 \\ 0 & 0 & 0 & k_{P_1} & 0 \\ 0 & 0 & 0 & 0 & k_{P_2} \end{bmatrix} \begin{bmatrix} e_{X,n} \\ e_{S_1,n} \\ e_{S_2,n} \\ e_{P_1,n} \\ e_{P_2,n} \end{bmatrix}}_{L} + T_S X_n \underbrace{\begin{bmatrix} \left.\frac{\mathrm{d}\mu_1(S_1,P_{1,n})}{\mathrm{d}S_1}\right|_{S_\theta} \\ 0 \\ 0 \\ -\left.\frac{\mathrm{d}q_{S_1/P_1}(S_1,P_{1,n})}{\mathrm{d}S_1}\right|_{S\varphi} \\ -\left.\frac{\mathrm{d}q_{S_1/P_2}(S_1,P_{2,n})}{\mathrm{d}S_1}\right|_{S\alpha} \end{bmatrix}}_{NL} e_{S_1,n}. \tag{22}$$

In Eq. (22), L is a linear system and NL is a bounded nonlinearity [19]. Note that if $k_\sigma = 0$, the reference is reached in one step. So, if $0 < k_\sigma < 1$, the tracking error tends to zero when $n \to \infty$ [19, 24].

Controller implementation

The control system diagram is shown in Fig. 2 and the mathematical procedure is summarized in the following steps:

Bayesian state estimators design

Knowledge and control of certain compounds during fermentation are essential because they provide information that allows the process to be modified when necessary [25]. Some variables, such as cell concentration, are determined by off-line laboratory analysis, limiting its use for control purposes. Although a specific on-line sensor could be available, this kind of hardware is usually expensive.

State estimation methods have been mostly focused on supply the lack of system measurements [26, 27]. Nowadays, there are a wide variety of state estimators, Ali et al. [28], classified them into six groups: Luenberger-based, Finite-dimensional system, Bayesian, Disturbance and fault detection, AI-based and Hybrid observers. Most of them need fermentation mathematical model to be applied.

As most fermentation mathematical models are not entirely reliable, Bayesian estimators based on Gaussian processes are proposed. The following procedure shows a reliable tool design for the biomass, alcohol, and glycerol concentrations estimation.

Every learning algorithm requires a set of training elements. This set of noisy experimental data, D, is constituted by k pairs of n-dimensional input vectors x_i (regression vector) collected in a nxk matrix $\mathbf{X}$, and k scalar noisy observed outputs y_i joined in a vector y; where k and n are the number of samples taken and known variables, respectively.

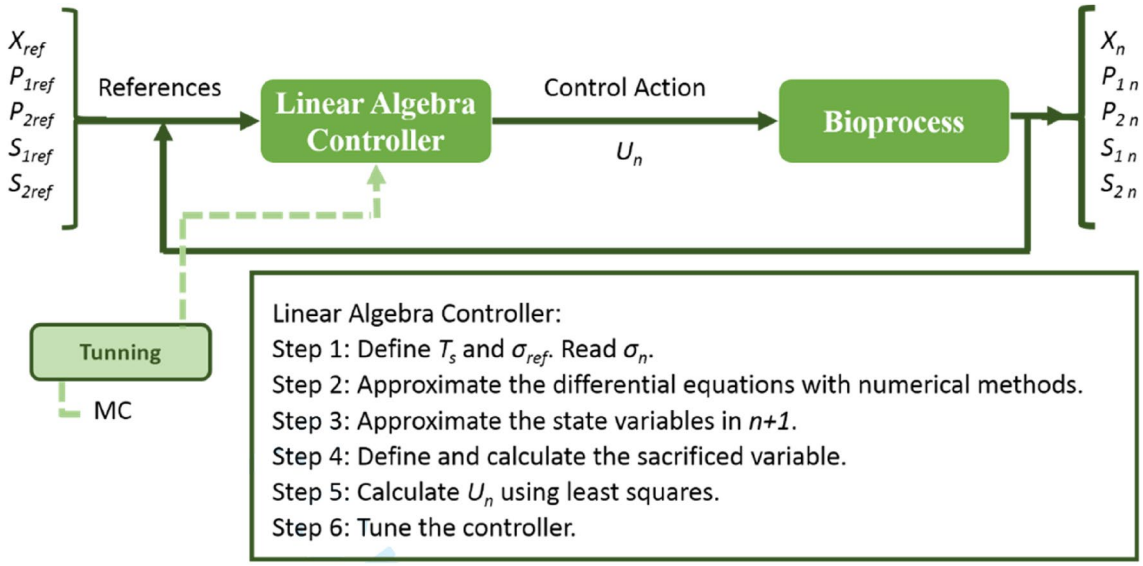

Fig. 2 Control system diagram

$$D = \left\{\left(x_i, y_i\right)/i = 1, \ldots, k\right\} = \{\mathbf{X}, y\}. \tag{23}$$

In this sense, the objective is to find y values corresponding to x* not included in **X**. For this, the following Gaussian regression model is constructed:

$$y_i = f\left(x_i\right) + \varepsilon_i. \tag{24}$$

In Eq. (24), y_i is the observed noisy outputs vector; $f(x_i)$ is the latent function (determines the relationship between the estimated variable and the data); ε_i is the additive noise (associated with measurement errors), usually represented by Gaussian white noise.

Then, $f(x_i)$ must be selected to make predictions for all possible inputs $x* \notin \mathbf{X}$, using the Bayes'rule (Eq. (25)) [29]. To achieve this goal, it is considered an infinite space of functions, each of them with a priori probability assigned, the highest probability are for those functions with certain characteristics (softness, stationariness, periodicity, etc.). Moreover, uncertainties are quantified by a posterior distribution. Equation (25) represents the application of Bayes'rule to the problem under study.

$$\overbrace{P(f_i|y)}^{\text{posterior}} = \frac{\overbrace{P(y|f_i)}^{\text{likelihood}}\overbrace{P(f_i)}^{\text{prior}}}{\underbrace{P(y)}_{\text{evidence}}} = \frac{P(y|f_i)P(f_i)}{\sum_{i=1}^{\infty} P(f_i)P(y/f_i)}. \tag{25}$$

Equation (25) updates a posterior distribution (predictive function) with the empirical data and the a priori distribution assumed over the space of the possible functions that model the input data. $P(f_i)$, expresses the type of function that is expected to be observed as output, e.g., continuous and smooth, those properties are induced by the covariance function (**K**) and is denoted as:

$$P(f_i) = N(0, \mathbf{K}) \tag{26}$$

$P(y/f_i)$ describes the deviation of the noisy measurements, y_i, respect of the free-noise function, $f(x_i)$. The likelihood is represented by:

$$P(y/f_i) = \prod_{i=1}^{m} N\left(f_i, \sigma_n^2\right) = N\left(f, \sigma_n^2 I\right). \tag{27}$$

The evidence, $P(y)$, is the normalizing constant and is calculated with the Total Probability Theorem that involves both terms, a priori probability, and likelihood.

Then, $P(f_i/y)$ is obtained by replacing Eqs. (26) and (27) in (25):

$$\begin{aligned} P(f_i/y) &\propto N\left(f, \sigma_n^2 I\right) N(0, \mathbf{K}) \\ P(f_i/y) &= N\left(\mathbf{K}\left(\mathbf{K} + \sigma_n^2 I\right)^{-1} y, \left(\mathbf{K}^{-1} + \sigma_n^2 I\right)^{-1}\right). \end{aligned} \tag{28}$$

Finally, considering a hypothetical case x*, to predict the value of $f*$ an average, overall possible functions, is evaluated from Eq. (28). In this way, the predictive function, $f*$, is given by:

$$P(f*/x*) = \int P(x*/f*)P(f)\mathrm{d}f. \tag{29}$$

Consequently, the problem of Bayesian estimation is reduced to find the appropriate properties for the covariance function, which depends on the Kernels functions

chosen to describe the curves and the determination of their hyperparameters.

Covariance function

The covariance function, **K**, is a degree and type measure of the relation of two variables. In this case, represents the correlation between the training input and output data, **X** and *y*. For a set of *n* variables:

$$\mathbf{K} = \begin{bmatrix} k(x_1, x_1) & \cdots & k(x_1, x_n) \\ \vdots & \ddots & \vdots \\ k(x_n, x_1) & \cdots & k(x_n, x_n) \end{bmatrix}. \tag{30}$$

Each component of **K** is formed by adding kernels. Several kernel functions describe different kinds of curves, Table 3 shows some of them [30]. As a result, there are many possibilities of covariance function, the only restriction is that this matrix must be symmetric and positive defined [31, 32].

Hyperparameters

Hyperparameters are parameters of a non-parametric model. They do not have a fixed value, previously established by adjusting a model; therefore, it is necessary to estimate them. To achieve this goal, they are defined as the logarithm of the covariance function variables, since they are positive scaling parameters.

There are many alternatives to solve the hyperparameters estimation: *general optimization of error limits* [33–35], *cross-validation method* [36], *evidence maximization* [37, 38], *Monte Carlo methods* [39], *maximum* a posteriori *method* [31, 40], and *maximum likelihood* [41].

Table 3 Función Kernel [30]

Constante	σ_0^2
Lineal	$\sum_{d=1}^{D} \sigma_d^2 x_d x'_d$
Polinomial	$\left(x \cdot x' + \sigma_0^2\right)^p$
Exponencial cuadrado	$\exp\left(-\frac{r^2}{2l^2}\right)$
Matérn	$\frac{1}{2^{\nu-1}\Gamma(\nu)}\left(\frac{\sqrt{2\nu}}{l}r\right)^{\nu} K_\nu\left(\frac{\sqrt{2\nu}}{l}r\right)$
Exponencial	$\exp\left(-\frac{r}{l}\right)$
γ-exponencial	$\exp\left(-\left(\frac{r}{l}\right)^{\gamma}\right)$
Racional cuadrático	$\left(1 + \frac{r^2}{2\alpha l^2}\right)$
Red neuronal	$\sin^{-1}\left(\frac{2\tilde{x}^T \sum \tilde{x}'}{\sqrt{(1+2\tilde{x}^T \sum \tilde{x})(1+2\tilde{x}'^T \sum \tilde{x}')}}\right)$

In this paper, the maximum a posteriori method is used. It consists of using Gaussian processes to carry out the hyperparameters search. This implies assuming an a priori distribution about hyperparameters, applying Bayes'rule and the other previously explained steps [42].

Implementación

There are four steps to follow:

- Regression vector selection.
- Latent function determination.
- Covariance function choose.
- Hyperparameters estimation.

Initially, the training data set is defined using different feed rate profiles:

$$D = \left\{\left(x_i, y_i\right)/i = 1, \ldots, k\right\} = \left\{P_1, P_2, S_1, S_2, X\right\} \tag{31}$$

The regression vectors for biomass, ethanol and glycerol estimation are:

$$\begin{aligned} R_X &= \left[S_{1i}\, S_{2i}\, X_{i-1}\, X_{i-2}\right] \\ R_{P_1} &= \left[S_{1i}\, S_{2i}\, P_{1_{i-1}}\, P_{1_{i-2}}\, S_{1i} P_{1_{i-1}}\right] \\ R_{P_2} &= \left[S_{1i}\, S_{2i}\, P_{2_{i-1}}\, P_{2_{i-2}}\, S_{1i} P_{2_{i-1}}\right]. \end{aligned} \tag{32}$$

Consequently, the following models of Gaussian regression for cell, ethanol, and glycerol data generation are proposed:

$$\begin{aligned} X_i &= \hat{X}_i + \varepsilon_i \\ P_{1i} &= \hat{P}_{1i} + \varepsilon_i \\ P_{2i} &= \hat{P}_{2i} + \varepsilon_i, \end{aligned} \tag{33}$$

where, $\hat{X}_i$, $\hat{P}_{1i}$ and $\hat{P}_{2i}$ are the latent functions.

Then, as the heart of Bayesian estimators lies in the determination of an appropriate covariance matrix, selected functions must: have high flexibility, consider different types of data interactions, harmonize the estimation results when the data is close or spaced, contemplate linear and non-linear relationships, present robustness against measurement errors, among others. Therefore, the covariance function selection requires in-depth knowledge of both the system under study and the different kernels that may constitute it.

In this sense, the covariance functions proposed by Williams and Rasmussen [43] and di Sciascio and Amicarelli [31] were analysed. As a main contribution, in this paper the following covariance function is proposed:

$$k_{x_{ij}} = \theta_0 + \theta_1 \exp\left[-\frac{1}{2}\sum_{\ell=1}^{n}\frac{\left(x_i^{(\ell)} - x_j^{(\ell)}\right)^2}{r_{a\ell}^2}\right] + \theta_2 \exp\left[-\frac{1}{2}\sum_{\ell=1}^{n}\frac{\left(x_i^{(\ell)} - x_j^{(\ell)}\right)^2}{r_{b\ell}^2}\right] + \ldots$$
$$\ldots + \theta_3\delta(i,j) + \sum_{\ell=1}^{n}\alpha_\ell x_i^{(\ell)} x_j^{(\ell)} \tag{34}$$

In Eq. (34), θ_0, $\theta 1$, r, $\theta 2$, θ_3 and α are the covariance function hyperparameters, δ is the Kronecker Delta function, and ℓ is the space dimension of x_i. The terms in Eq. (34) are briefly described:

- First term: is called bias, and it reflects how far the average inference function is expected to fluctuate from the average of the Gaussian process.
- Second and third terms: are square exponential kernels, they express that close inputs give rise to close outputs. r_ℓ is the characteristic scalar length (establishes how far the input values, x_i, can be for estimated values, y_i, become uncorrelated) and θ_1 and θ_2 provide general vertical scale regarding the average of the Gaussian process output space. It is one of the most used kernels in bioprocesses, because it provides softness characteristics, achieving an excellent curves description.
- Fourth term: represents white noise, corresponding, e.g., to measurements impressions. θ_3 is the noise variance.
- Fifth term: is a linear kernel and is the non-stationary part of the covariance function. The amount of hyperparameters it has α coincides with the size of the regression vector.

Once the covariance function is defined, the hyperparameters vector is determined:

$$\theta \triangleq \left[\log\theta_0, \log\theta_1, \log r_{a1}, \ldots, \log r_{an}, \log\theta_2, \log r_{b1}, \ldots, \log r_{bn}, \log\theta_3, \log\alpha_1, \ldots, \log\alpha_n\right]. \tag{35}$$

In this case, there are 16 hyperparameters to be determined for biomass, *9* for ethanol and 19 for glycerol estimators.

To implement the Bayesian estimation algorithms, an open-source toolbox of MatLab™ called *GPML* (Gaussian Process for Machine Learning) is used. In Rasmussen and Nickisch [44], this tool is described. Then, the Total Error, Eq. (12) is used to evaluate the estimators performance. Figure 3 shows a flowchart of the proposed procedure.

Results and discussion

In this section, the results of coupling the estimators and the linear algebra controller are shown. The estimated variables are cell, ethanol, and glycerol concentrations throughout the process. Initially, the control loop is tested under normal operating conditions, then parametric uncertainty and disturbances in the control action are added to demonstrate the reliability of the control strategy and the proposed estimators. Besides, in all cases, the results are compared and contrasted with those obtained with the previously published neuronal network estimators.

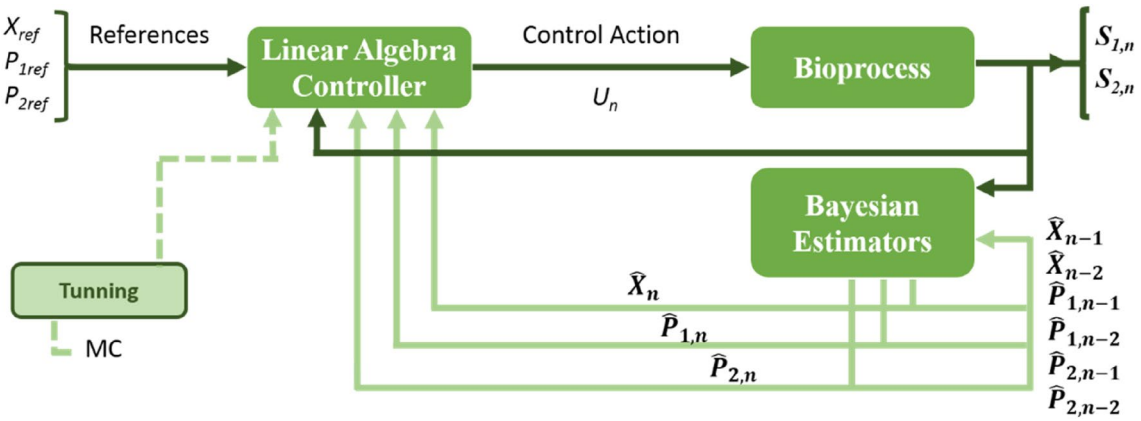

Fig. 3 Process flowchart

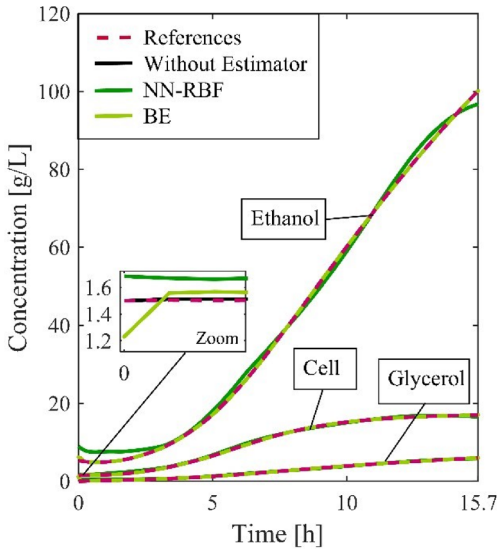

Fig. 4 Cell, ethanol, and glycerol concentration obtained by coupling the estimators to the controller under normal operating conditions

Performance under normal conditions

This test tries to simulate how the system would behave when no external factors affect the process. Figure 4 shows the evolution of cell, ethanol, and glycerol reference concentration profiles, those obtained with the neuronal network estimator (NN-RBF), the Bayesian estimator (BE) and those that would be ideal (without estimator). Note the good performance of both kinds of estimators; however, there is an improvement in the results when using the Bayesian estimator.

Figure 5 describes the accumulated error and the tracking error obtained with each estimator and in ideal conditions (without estimator). The neural network introduces a limited intrinsic error that is accumulated along the process, so the accumulated error is different from that of the Bayesian estimator. As can be seen, as the process progresses, the tracking error tends to decrease and remains limited to low values, that is, the controller progressively approaches the reference at every instant of time.

Performance with parametric uncertainties

A particular characteristic of bioprocesses is the difficulty of measuring their parameters, especially since they often vary over time [45]. Therefore, the following test attempts to show how the controller and estimators respond when the system parameters values are not accurate or fluctuate throughout the process.

To achieve this goal, the Monte Carlo algorithm is used. The number of simulations (N) is determined with Eq. (10), taking into account the same confidence and accuracy values as in Sect. Controller tuning. Among the N simulations, all system parameters are randomly changed by $\pm 15\%$ of their original value at the same time. Figure 6 shows the biomass concentrations obtained in the 1000 simulations with parametric uncertainty when using the Neural Network and Bayesian estimator; while Figs. 7 and 8 the results for ethanol and glycerol concentrations, respectively. Note that

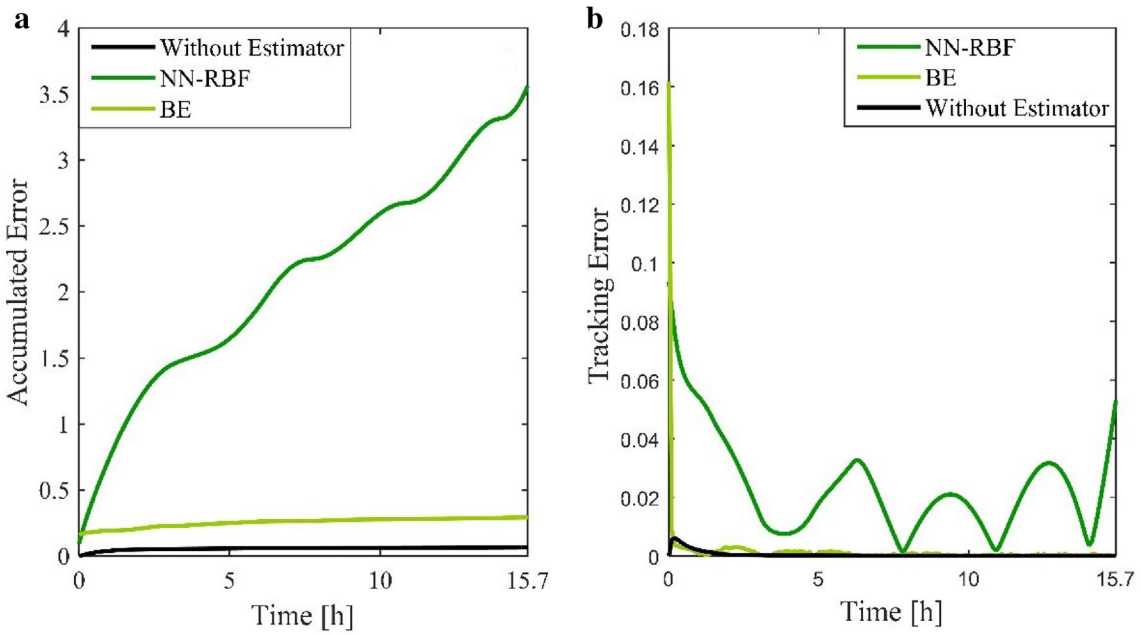

Fig. 5 **a** Accumulated error and **b** tracking error obtained by coupling the estimators to the controller under normal operating conditions

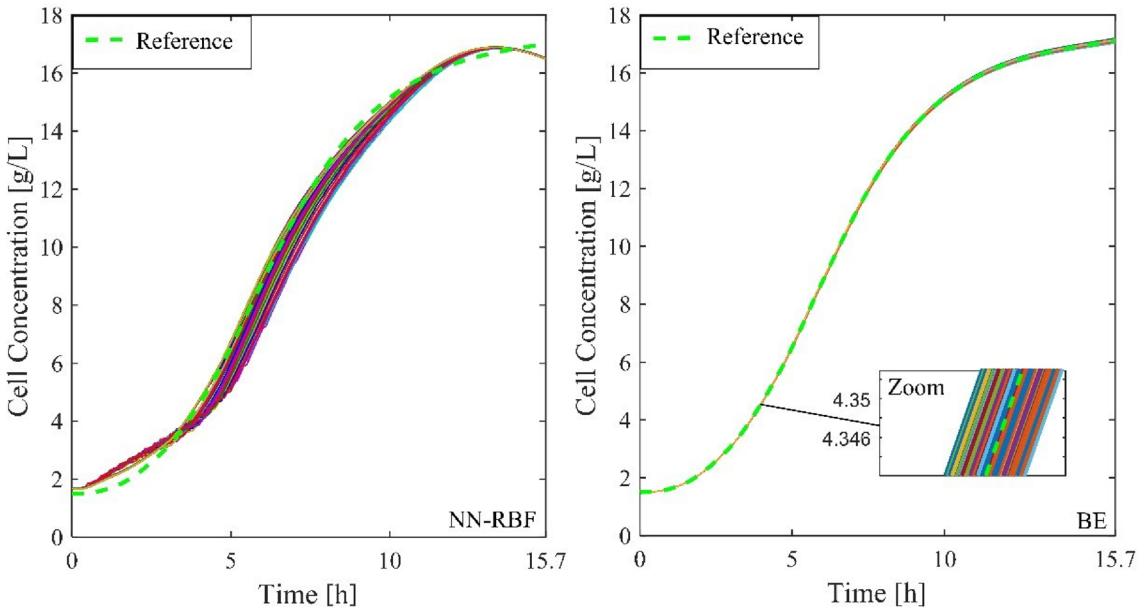

Fig. 6 Cell concentration variation under parametric uncertainty

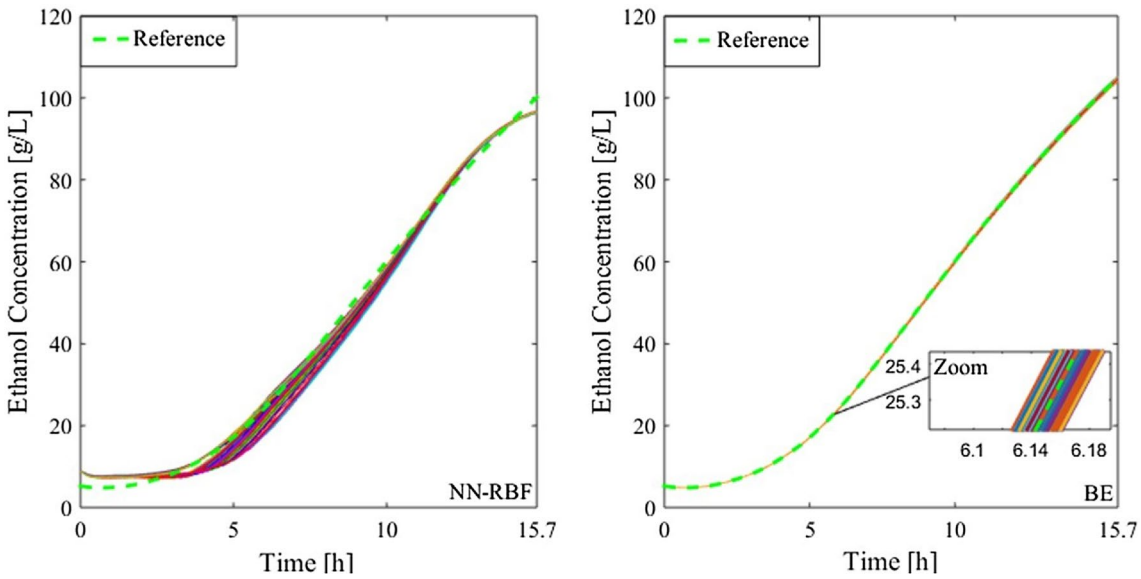

Fig. 7 Ethanol concentration variation under parametric uncertainty

the obtained profiles are acceptably close to each reference, especially those achieved with the Bayesian estimator.

Performance with disturbances in the control action

This test aims to simulate unforeseen events that can cause unwanted variations in production. To carry it out, a random disturbance is added to the bioreactor feed rate. This disturbance affects the control action in ± 20% of its original value. This can be explained as a random noise that results in Gaussian disturbances with non-zero average [46]. Figure 9 shows the disturbed feed speed profile in comparison to the reference. Figure 10 illustrates the reference concentration monitoring when using both state estimators coupled to the controller, despite the perturbation applied; finally, it can be observed how these disturbances cause an increase in the tracking error (concerning the one analyzed in Fig. 5), however, it remains at acceptable levels.

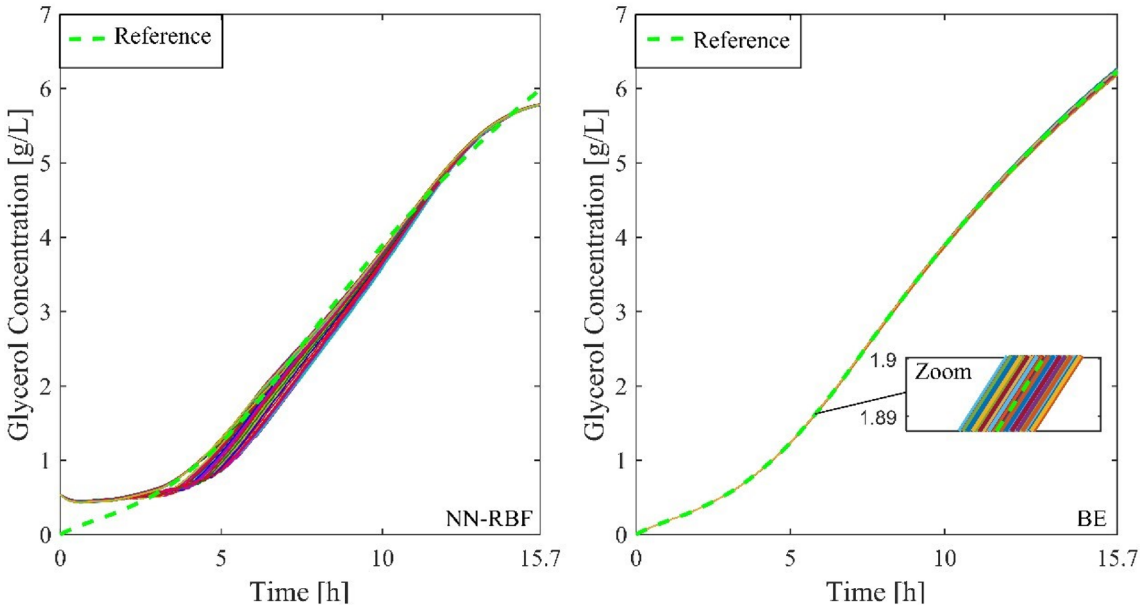

Fig. 8 Glycerol concentration variation under parametric uncertainty

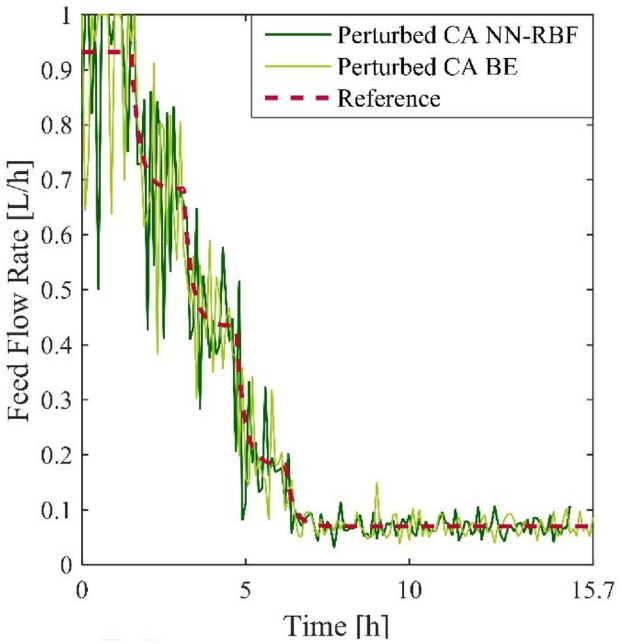

Fig. 9 Control Action with random perturbances

Conclusions

Reliable control strategies are fundamental for bioprocess good performance. For most of these strategies, knowledge of on-line states variables is necessary. Moreover, as specific on-line sensors are generally not available, relevant variables are usually measured by off-line methods, which require long-time analysis, preventing corrective action from being taken.

As a solution, in this paper, a controller design based on linear algebra for a multivariable and non-linear system is proposed. Furthermore, Bayesian state estimators based on Gaussian processes were proposed to estimate on-line cell, ethanol, and glycerol concentrations, using only substrates on-line measurement. As a main contribution, a new alternative of covariance function was presented, which allows reducing estimation errors.

The algorithms were applied in a fed-batch bioethanol fermentation process. The controller was tuned using the Monte Carlo algorithm. The controller with the estimator

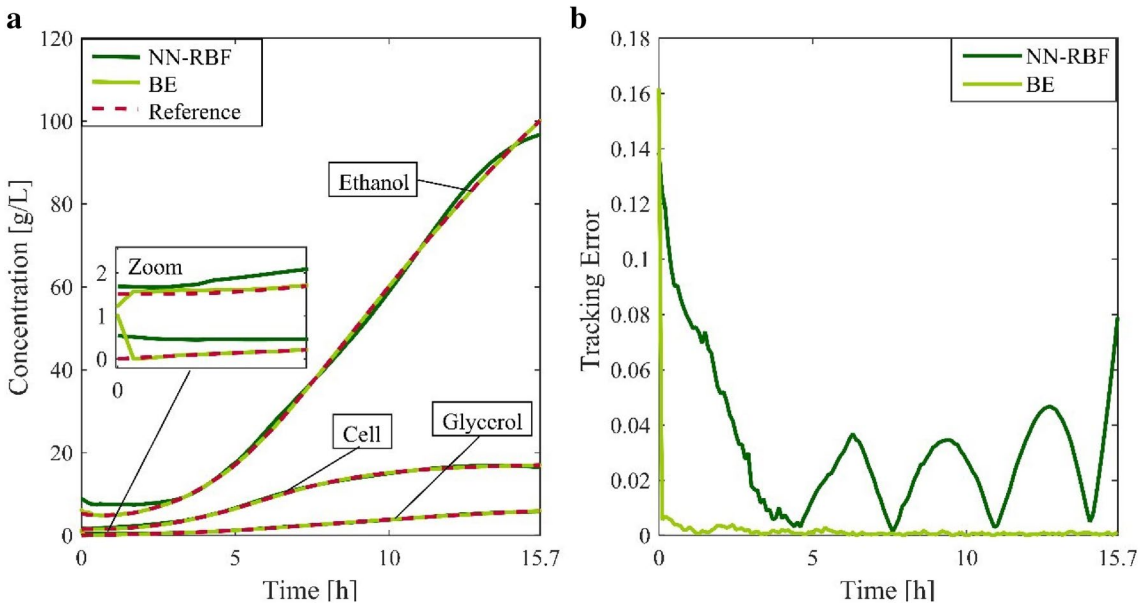

Fig. 10 **a** Cell, ethanol and glycerol concentrations profiles with perturbations in the control action. **b** Tracking error

coupled was tested under parametric uncertainty and disturbances in the control action. Each result was compared and contrasted with those obtained with neural network estimators, showing better results. Moreover, in the Bayesian estimator fewer parameters are involved, simplifying the mathematical resolution of the problem, reducing the programming time and minimizing the computational cost. Bayesian estimators show a performance improvement, which is reflected in a decrease of the total error. This last assertion is because the neural network introduces a limited intrinsic error that is accumulated along the process.

Acknowledgments To the National Council of Scientific and Technological Research (CONICET) and the Chemical Engineering Institute (IIQ) from the National University of San Juan for their support in this investigation.

Declarations

Conflict of interest All authors declare that they have no conflicts of interest.

References

1. Azhar SHM, R Abdulla SA Jambo H Marbawi JA Gansau AAM Faik 2017 Yeasts in sustainable bioethanol production: a review. Biochem Biophys Rep 10 52 61
2. de Azevedo A, Fornasier F, da Silva Szarblewski M, de Souza Schneider RDC, Hoeltz M, de Souza D (2017) Life cycle assessment of bioethanol production from cattle manure. J Clean Prod 162:1021–1030
3. Ozdingis AGB, Kocar G (2018) Current and future aspects of bioethanol production and utilization in Turkey. Renew Sustain Energy Rev 81:2196–2203
4. Vohra M, Manwar J, Manmode R, Padgilwar S, Patil S (2014) Bioethanol production: feedstock and current technologies. J Environ Chem Eng 2:573–584
5. Herrero ML, Vallejo MD, Sardella MF, Deiana AC (2015) Acid pretreatment of two phase olive mill waste to improve bioavailable sugars: conditions optimization using response surface methodology. Waste Biomass Valor 6:37–44
6. Aimaretti NR, Ybalo CV, Rojas ML, Plou FJ, Yori JC (2012) Production of bioethanol from carrot discards. Bioresour Technol 123:727–732
7. Kumar S, Dheeran P, Singh SP, Mishra IM, Adhikari DK (2015) Continuous ethanol production from sugarcane bagasse hydrolysate at high temperature with cell recycle and in-situ recovery of ethanol. Chem Eng Sci 138:524–530
8. Tgarguifa A, Abderafi S, Bounahmidi T (2017) Modeling and optimization of distillation to produce bioethanol. Energy Proc 139:43–48
9. Scaglia GJ, Aballay PM, Mengual CA, Vallejo MD, Ortiz OA (2009) Improved phenomenological model for an isothermal winemaking fermentation. Food Control 20:887–895
10. Ochoa S (2016) A new approach for finding smooth optimal feeding profiles in fed-batch fermentations. Biochem Eng J 105:177–188
11. Liu C, Gong Z, Shen B, Feng E (2013) Modelling and optimal control for a fed-batch fermentation process. Appl Mathl Modelling 37:695–706
12. Jin H, Chen X, Yang J, Wu L, Wang L (2014) Hybrid intelligent control of substrate feeding for industrial fed-batch chlortetracycline fermentation process. ISA Trans 53:1822–1837
13. Mandenius C-F (2004) Recent developments in the monitoring, modeling and control of biological production systems. Bioprocess Biosyst Eng 26:347–351
14. Hussain M, Ramachandran K (2002) Comparative evaluation of various control schemes for fed-batch fermentation. Bioprocess Biosyst Eng 24:309–318

15. Huang D, Lv J (2020) Run-to-run control of batch production process in manufacturing systems based on online measurement. Comput Ind Eng 141:106298
16. Liu K, Chen Y, Zhang T, Tian S, Zhang X (2018) A survey of run-to-run control for batch processes. ISA Trans 83:107–125
17. Baeza JA (2017) 18—principles of bioprocess control A2—Larroche, Christian In: Sanromán MÁ, Du G, Pandey A (eds) Current developments in biotechnology and bioengineering. Elsevier, pp 527–561
18. Hunag W-H, Shieh GS, Wang F-S (2012) Optimization of fed-batch fermentation using mixture of sugars to produce ethanol. J Taiwan Inst Chem Eng 43:1–8
19. Fernández MC, Nadia Pantano M, Rossomando FG, Alberto Ortiz O, Scaglia GJ (2019) State estimation and trajectory tracking control for a nonlinear and multivariable bioethanol production system. Brazil J Chem Eng 36:421–437
20. Griffiths DV, Smith IM (2006) Numerical methods for engineers. CRC Press
21. Strang G (2005) Linear algebra and its applications. Thomson Brooks/Cole, Belmont, CA, USA
22. Tempo R, Ishii H (2007) Monte Carlo and Las Vegas randomized algorithms for systems and control: an introduction. Eur J Control 13:189–203
23. Puchol MCF, Pantano MN, Godoy S, Serrano E, Scaglia G (2018) Optimización de Parámetros Utilizando los Métodos de Monte Carlo y Algoritmos Evolutivos. Aplicación a un Controlador de Seguimiento de Trayectoria en Sistemas no Lineales," *Revista Iberoamericana de Automática e Informática industrial,* 2018
24. Scaglia G, Rosales A, Quintero L, Mut V, Agarwal R (2010) A linear-interpolation-based controller design for trajectory tracking of mobile robots. Control Eng Pract 18:318–329
25. Mentana A, Palermo C, Nardiello D, Quinto M, Centonze D (2012) Simultaneous and accurate real-time monitoring of glucose and ethanol in alcoholic drinks, must, and biomass by a dual-amperometric biosensor. J Agric Food Chem 61:61–68
26. Salau NP, Trierweiler JO, Secchi AR (2012) State estimators for better bioprocesses operation. In: Computer aided chemical engineering, vol. 30. Elsevier, pp 1267–1271
27. Assis A, Maciel Filho R (2001) Control applications of artificial neural networks in bioprocessing and chemical engineering: a review. In: First Mercosul Congress On Chemical Engineering-Empromer, 2001, pp 361–366
28. Ali JM, Hoang NH, Hussain MA, Dochain D (2015) Review and classification of recent observers applied in chemical process systems. Comput Chem Eng 76:27–41
29. Bernardo JM, Smith AF (2009) Bayesian theory, vol. 405. Wiley
30. Bergman S, Schiffer M (2005) Kernel functions and elliptic differential equations in mathematical physics. Courier Corporation
31. Sciascio di F, Amicarelli AN (2008) Biomass estimation in batch biotechnological processes by Bayesian Gaussian process regression. Comput Chem Eng 32:3264–3273
32. Abrahamsen P (1997) A review of Gaussian random fields and correlation functions. In: Norsk Regnesentral/Norwegian Computing Center Oslo, 1997
33. Chapelle O, Vapnik V (2000) Model selection for support vector machines. In: Advances in neural information processing systems, pp. 230–236
34. Cristianini N, Campbell C, Shawe-Taylor J (1999) Dynamically adapting kernels in support vector machines. In: Advances in neural information processing systems, pp 204–210
35. Schölkopf B, Bartlett PL, Smola AJ, Williamson RC (1999) Shrinking the tube: a new support vector regression algorithm. In: Advances in neural information processing systems, pp 330–336
36. Wahba G (1999) Support vector machines, reproducing kernel Hilbert spaces and the randomized GACV. Adv Kernel Methods-Support Vect Learn 6:69–87
37. Gibbs MN (1998) Bayesian Gaussian processes for regression and classification. Citeseer
38. MacKay DJ (1992) A practical Bayesian framework for backpropagation networks. Neural Comput 4:448–472
39. Neal RM (1997) Monte Carlo implementation of Gaussian process models for Bayesian regression and classification. *arXiv preprint physics/9701026,* 1997
40. Rasmussen CE (1997) Evaluation of Gaussian processes and other methods for non-linear regression. University of Toronto, Toronto
41. Akaike H (1998) Likelihood and the Bayes procedure. In: Selected papers of Hirotugu Akaike. Springer, pp 309–332
42. Rómoli S, Amicarelli AN, Ortiz OA, Scaglia GJE, Sciascio di F (2016) Nonlinear control of the dissolved oxygen concentration integrated with a biomass estimator for production of *Bacillus thuringiensis* δ-endotoxins. Comput Chem Eng 93:13–24
43. Williams CK, Rasmussen CE (1996) Gaussian processes for regression. In: Advances in neural information processing systems, pp 514–520
44. Rasmussen CE, Nickisch H (2010) Gaussian processes for machine learning (GPML) toolbox. J Mach Learn Res 11:3011–3015
45. Wechselberger P, Seifert A, Herwig C (2010) PAT method to gather bioprocess parameters in real-time using simple input variables and first principle relationships. Chem Eng Sci 65:5734–5746
46. George J (2014) On adaptive loop transfer recovery using Kalman filter-based disturbance accommodating control. Control Theory Appl IET 8:267–276